

# FRAMEWORK FOR CEMENTED TUNGSTEN CARBIDE DRILL BIT PROTOTYPE FABRICATION USING LASER ENGINEERED NET SHAPING

Brandon Davoren

*Department of Industrial Engineering  
& DSI-NRF Centre of Excellence in  
Strong Materials  
Stellenbosch University  
Stellenbosch, South Africa  
brandond@sun.ac.za*

Natasha Sacks

*Department of Industrial Engineering  
& DSI-NRF Centre of Excellence in  
Strong Materials  
Stellenbosch University  
Stellenbosch, South Africa  
natashasacks@sun.ac.za*

Maritha Theron

*National Laser Centre  
Council for Scientific and Industrial  
Research  
Pretoria, South Africa  
mtheron@csir.co.za*

**Abstract**— The interest in additive manufacturing and its unique applications has increased significantly over recent years. This has resulted in the need for alloys and composites to be optimized for these processes. In this study a multiphase parameter refinement framework was developed to guide optimization, and a cemented tungsten carbide alloy was used as a means of validation. Laser engineered net shaping (LENS<sup>TM</sup>) was used to fabricate thin walls, cubes, and a functional prototype, namely a drill bit. The circularity, depth and diameter of the drilled holes were benchmarked against a commercially available drill bit, and finite element modelling simulations were performed to illuminate regions of high stress and indicate possible fracture zones. The circularity of the resultant holes was found to be consistent for the respective drill bits except when the drill bit tip failed and tore material from the walls of the hole. The depth and diameter of the drilled holes varied across the tests and the depth was significantly less for the fabricated drill bits compared to the commercial drill bit. The framework allowed for the functional prototype to be fabricated in 23.5 hours of active laser time. A second iteration of the refinement stage or redesign of the component could lead to improved drilling performance and will be considered in future studies.

**Keywords**—laser engineered net shaping, framework, cemented tungsten carbide, drill bit, design of experiments

## I. INTRODUCTION

Limited commercialization, including research, has been done using the DED process to manufacture cemented tungsten carbides, with only cobalt (Co) being utilized as a binder phase [1]. Since DED has been used to develop, prototype and produce specialized surgical prosthetics [2] it therefore has the potential to fabricate precision drilling tools. If additive manufacturing (AM) methods can be utilized to fabricate drill bits then custom bits can be printed on demand for specialized applications without the need to mass produce, as is the case with modern commercial manufacturing methods. Furthermore, if a drill bit becomes worn or fractures, it could potentially be rebuilt or repaired using an AM process instead of purchasing a new drill bit. Thus, the focus of the current study was to produce cemented tungsten carbide drill bit prototypes using the DED process, and to compare initial drilling performance against a commercially available drill bit.

To produce successful AM prototypes an optimized manufacturing framework is required. In literature an AM component is generally fabricated using an optimal set of parameters with limited information provided on how these parameters were obtained [3], [4]. Attempts to duplicate the component are often only feasible if there is an abundance of information available regarding the process parameter optimization process which was followed for successful material deposition, which is only the case for commonly printed materials such as titanium based alloys [5]. However, there is not always published parameters or manufacturing frameworks to aid the deposition process when novel alloys or binders are considered, or even when AM is considered as an alternative production process for an existing material such as cemented tungsten carbide. A framework which allows for rapid parameter optimization is required for these instances, or a critical simulation study can also be undertaken. Researchers have used a design of experiments matrix to develop the optimization process [6], although a basic framework for parameter optimization using an iterative deposition approach is not readily available, which would also assist researchers new to the field of additive manufacturing as well as in the development of novel alloys.

Therefore, based on the high number of depositions required and the absence of a published basic optimization framework, a simple framework was designed in this study which used multiple simple cubic geometries to determine an optimal parameter set which could be used for the deposition of a functional prototype. It also determined whether parameters obtained for various geometries could be simply translated across designs. The LENS<sup>TM</sup> fabricated WC-9.2wt% Monel400 drill bits were tested against a commercially available product to determine whether the additively manufactured prototype was comparable. Here the entire drill bit comprised of the cemented carbide whereas the shank of the purchased drill bit is fabricated from steel and only the tip region from WC-based materials. The study aimed to achieve these results by using the least number of depositions and total laser time. The framework can be utilised in any experimental setup where a novel material combination is required to be optimised.

## II. FRAMEWORK FOR PROTOTYPING DRILL BITS

Design of experiments (DoE) and statistical based approaches have been used by numerous researchers [7]–[9] to provide valuable information for the generation of numerical models, machine learning parameter optimizers and finite element analysis models. The framework developed in this study was based on these approaches with adaptations made to the optimization process to produce a functional prototype. It is also provided in a simple layout such that it can be applied in any iterative parameter testing situation. The proposed framework is shown in Fig. 1 and can be used to optimize the parameters for the deposition of a functional prototype, by starting with thin walls and then optimizing through small-scale samples. The framework is divided into several phases which are discussed in more detail thereby providing a general overview and the approach used in this study.

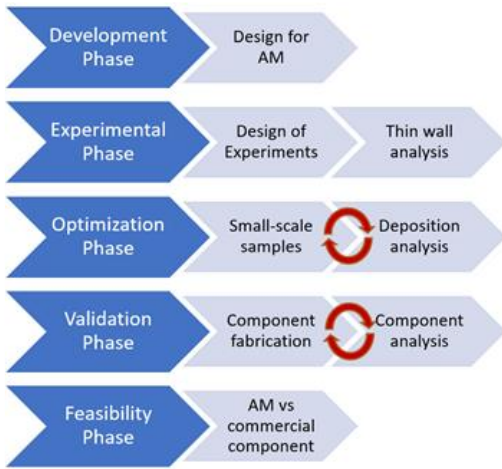


Fig. 1: Framework for drill bit prototype fabrication

### A. Development phase

#### 1) Design for AM

Design for Additive Manufacturing (DfAM) has the highest impact for production parts and the lowest for a prototype since the time spent optimizing a production part will be justified in the reduction of batch material waste and time reduction. The design process is therefore a crucial stage in additive manufacturing and has been explored by multiple authors [10], [11]. The design stage undergoes an iterative approach [12] until the model meets the desired requirements which could include reduction of build material and localized stresses, by using generative design, appropriate angular structures or the addition of support structures. The conceptualization of the component needs to accommodate the limitations of the additive manufacturing technology to be used as well as maintain the desired features without extensive compromise. Salonitis and Zarban [12] presented a simple and definitive hierarchical and multi-criteria decision making design for choosing an optimized design. The drill bit prototypes, in this study, were modelled using the commercial drill bit as a template since the benchmarking was performed against the commercial bit.

### B. Experimentation phase

#### 1) Design of experiments

Design of experiments have been used by multiple researchers to perform optimization experiments [6], [13]. Many experimental design templates are available within statistical software and are calibrated using the desired outcomes of the study. Two examples of widely used design of experiments are Factorial and Taguchi designs. Factorial based designs consider all possible interactions that occur for each of the input factors which results in large experimental sets. Factorial designs allow for interactions between parameters to be determined although one pitfall is that some interactions may be confounded and if not considered can lead to highly erroneous conclusions. Taguchi designs are based on fractional factorial designs as well as factorial designs with multiple factors being tested. With Taguchi designs, the most significant interactions need to be hypothesized before the experimental processes commence. A design of experiments allows for analysis of variance (ANOVA) to be applied to the obtained experimental data and provide results which pertain to the experimental range employed. Any variable sets which are beyond the scope of the study can be extrapolated although this assumes that the mathematical nature of the results is consistent over any variable set, which is not necessarily true. When a novel material is the subject of the research and no defined literature is available, then other materials which have been used for the intended application or the major alloying substituents can provide a guideline as to how the material may react and provide beneficial properties such as hardness, strength and layer thickness in determining feasible initial parameter sets.

For this study, a 3x3 full factorial DoE was used including star points. The range which was chosen was hypothesized to contain a local “optimized” set which cannot be defined as a globally “optimized” set due to the restrictive nature of the design of experiments. Only three important parameters were considered in the design of experiments as not all parameters can be tested due to the exponential effect an additional parameter has on the number of depositions required. The laser beam power, traverse speed and powder flow rate were selected since literature has identified these as the main deposition parameters [14]. Three values / settings at a low, medium and high level, relative to the maximum and minimum of the machine, for each parameter yields a 3x3 matrix. Three levels provide more information about the interactions of the parameters and the inclusion of star points provides more information about the parameter sets around the “central” values of the design matrix. The values in Table I, along with the 6-star points resulted in 33 depositions.

TABLE I. VALUES USED IN CONSTRUCTING THE DESIGN OF EXPERIMENTS MATRIX.

Deposition Parameters			
Laser beam power (W)	Traverse Speed (mm/s)	Powder flow rate (g/min)	z-increment (mm)
150, 250, 350	2, 3, 4	5, 7.5, 10	0.2

Thin walls provide an ideal deposition design for rapid variable set determination due to low deposition times. The thin walls were 20 mm in length, 25 layers high and on a

single deposition track. A schematic of the thin wall depositions is shown in Fig. 2 (a).

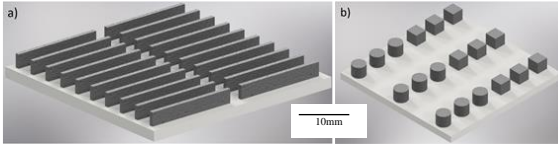


Fig. 2: General schematic for a) design of experiments thin walls b) cubic and cylindrical structures

## 2) Thin wall analysis

Once the thin walls have been deposited analysis needs to be performed such that feasible parameters can be obtained for the optimization phase. If there are any visible cracks, agglomerated particles causing surface roughness, poor adherence to the base plate or insufficient build height in the depositions then the parameter sets should be excluded. The properties of interest should be recorded, such as height, width or porosity for each parameter set so that an analysis of variance can be performed and the effect of each parameter as well as parameter interactions can be determined for the desired property. The desired parameter set is then used in the optimization phase with small-scale depositions.

The height, width and hardness were analysed and recorded for the 33 DoE trials. The theoretical height and width of the thin walls were calculated using the z-increment and beam spot size, respectively. An ANOVA regression and the resultant quadratic function was used to determine the most feasible parameter set, for the optimization phase. The parameter contributions and interactions in yielding a specific height, width and hardness were also analysed.

## C. Optimization phase

### 1) Small-scale samples

Small-scale samples can now be used to test the best parameter sets obtained from the experimentation phase. Small cubes or cylinders, as in Fig. 2(b), can be deposited and have been used in multiple publications as an optimization standard and many researchers use these as a base to subtractively machine tensile components [15]. The samples are now larger than thin walls and filled with a rastering pattern which introduces different thermal gradients and cooling rates during deposition which allows for the parameter sets to be refined further. The set which performed best on the thin walls may not be the best solution for filled geometries but provide a feasible starting point. There are many parameters which can be altered such as hatch rastering pattern, z-increment, laser beam working distance, spot size and hatch overlap which will change the properties of the final deposition. The thin walls were deposited at a certain laser beam spot size and working distance for the parameter sets to thus translate more efficiently; these should be kept consistent. Depending on the results obtained for the deposition analysis, different parameters are changed for each iteration until the required physical or chemical property is obtained.

In this study three iteration phases were performed. The first consisted of the laser beam power, traverse speed and powder feed rate being altered although maintaining a fixed energy density [16] according to Equation 1, as determined from the design of experiment phase with a hatch overlap of

50% and 75%, beam spot size of 1.35 mm and z-increment of 0.2 mm.

$$P/vD = E \quad (1)$$

where P is the laser power (W or J/s), v is the scanning speed (mm/s) of the operating head, D is the diameter (mm) of the laser spot and E is the energy density (J/mm<sup>2</sup>).

The second iteration used the parameter set from the first iteration which yielded the lowest porosity. Different powder feed rates and z-increments were condensed into a single iteration to reduce redundant testing. The third iteration consisted of minor alterations to the hatch overlap and z-increment with the intention of reducing the final porosity.

### 2) Deposition analysis

The final intended use of the component or aim of the research study will determine the analysis performed and desired optimization which will be obtained through the iterative process. Tensile strength, fracture toughness, microstructure, hardness or density are some of the properties that are of interest in the current application [17].

The porosity was chosen as the deciding factor in the number of iterations required, as it was found to be a critical factor during deposition analyses. The porosity was measured for each of the samples of the iteration by analysing microscopy images and based on the values, the viability and necessity of the next iteration was determined. The parameter changes which would reduce the porosity were hypothesized based on whether porosity or lack-of-fusion was observed [18]. The hardness, chemical composition and microstructures were characterised in an earlier work [19] and used to understand and optimise the deposition process with greater confidence.

## D. Validation phase

### 1) Component fabrication

The optimized parameter set obtained from the optimization phase can now be applied to the validation phase. If the relative dimensions of the final component are the same as the small-scale sample, then the final CAD design can be applied in the optimization phase and optimized accordingly, or the CAD for the final product can be applied in this validation phase. The final component is however generally larger than the small-scale samples utilized in the optimization stage, which will affect the resultant cooling rates and thermal gradients during the deposition process [20]. It is important to monitor the first component print process to determine whether in-situ parameter adjustments are required to prevent the damage of the equipment, such as the deposition nozzle colliding with the build. These altered parameters can then be applied to the successive deposition process. According to Equation 1, the laser power and traverse speed directly affect the energy density. By lowering the laser power, the powder being fed may not melt adequately and result in lack of fusion porosity, whereas the higher traverse speed will yield less time at each successive point and may also develop porosity. A higher traverse speed is favourable over a lower laser power since this aids in faster printing, limiting layer thickness and reduces the alterations required to other parameters [21].

Based on the quality control minor changes can be made to the deposition parameters to improve the final product through the same iterative process used in the optimization phase. Additional post processing techniques can be employed such as Hot Isotactic Pressing (HIP) to reduce the porosity, surface finishing techniques to improve surface roughness or machining processes to enhance features of the final design. If none of these processes show a beneficial change or cause the product cost to elevate excessively then a new alloy should be examined for the process or a different manufacturing process or application should be investigated. The CAD of the drill bit for this study and an as-printed drill bit example is shown in Fig. 3(a) and Fig. 3(b) respectively, as was deposited using the process parameters recorded in Table II, along with a fixed powder feed rate of 11.9 g/min. The traverse speed was the only parameter altered to accommodate for the varied thermal properties and two drill bits were built on a heated stage to determine the effect on the deposition process. All drill bits except DB4 underwent mild sharpening after fabrication. Post processing is required to provide final products.

TABLE II. PRINTING PARAMETERS FOR DRILL BITS

Deposition Parameters				
Drill bit	Power (W)	Traverse speed (mm/s)	Substrate	Fabrication time (min)
1	220	8.2	Heated 450°C	100
2	220	10.25	Heated 450°C	60
3	220	20.50	Not heated	27
4	220	10.25	Not heated	40

## 2) Quality control

The component which is fabricated can be observed for any external anomalies such as insufficient build height, irregular surface agglomerates, high surface roughness, diminished components resolution or visible cracks. The samples can also be examined for porosity, micro cracks, hardness and various microstructural characteristics if necessary. Various failure criterion simulations can be applied to determine possible fracture sites and yield properties, such as Von Mises stresses [22].

The drill bits were printed without an iterative refinement step or post processing techniques such that the performance of the as-deposited prototype could be determined.

## E. Feasibility phase

This is concerned with the volume that needs to be printed, the time to print each component and the cost of the final part. After validation a full cost analysis needs to be applied to the final product to determine whether additive manufacturing is in fact the most cost efficient and suitable method for part production. Additive manufacturing has its strengths in low volume, highly customizable components, prototyping and concept validation. If high volume is required, then additive manufacturing can be used to design a mould which will allow for rapid manufacturing thereafter using injection moulding or metal casting. When accurate features and surface finish is required, a subtractive manufacturing process may be more suitable or even a different type of additive manufacturing process such as metal binder jetting.

The drilled hole quality was used for comparison against a commercial product. The drill bits were tested on a turn-mill at a rotational speed of 2000 rpm, a penetration depth of 6 mm with a feed rate of 100 mm/min. The holes were drilled into 2011 aluminium alloy which has a hardness of 90-100 HV<sub>0.1</sub>. Drilled hole circularity was analysed using image analysis software.

## III. FRAMEWORK VALIDATION

The powders and LENS™ configuration described in a previous study by Davoren et al. [19] was used in the framework validation. The study considered the design of experiments and optimization phase of a WC-9.2wt% Monel alloy, where the power and powder feed rate had a positive effect on the build height whereas the traverse speed and square of the powder feed rate had a negative effect, with power and powder feed rate showing antagonistic property data. The calculated model was found to explain the experimental data with 91.7% accuracy [19]. When the width was considered, an increase in laser power deposited a wider wall whereas a higher traverse speed deposited a thinner wall. Laser power and traverse speed were found to have an antagonistic effect and the calculated model was found to explain the experimental data with 93.2% accuracy.

The design of experiment phase provided important interactions and based on the calculated models allowed for cubes to be produced in the optimization phase. A density of 94% was obtained for the first iteration of the optimization phase, with the second yielding a density of 97% [19]. The third iteration did not reduce the porosity to any greater degree. In the current study the validation phase was done and used to produce a drill bit prototype based on the parameter set that yielded the 97% density, which is slightly lower than commercial densities of about 99%.

When the deposition properties are considered, it is evident from Fig. 3 (b) that the surface finish of the drill bit was very rough when compared to the CAD design in Fig. 3(a), due to the WC particles which did not dissolve and merely cooled in the binder while protruding from the deposition. The size of the WC powder particles ( $\pm 90 \mu\text{m}$ ) meant that if two or three particles are solidified upon one another, the surface roughness would increase. The nature of the precursor powder is therefore extremely important in

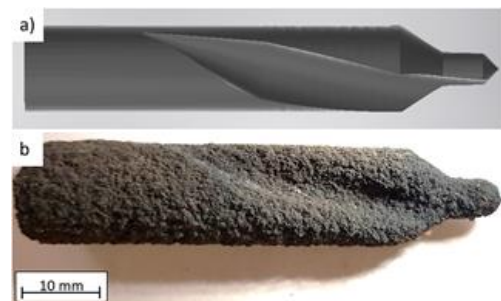


Fig. 3: a) CAD model of drill bit, b) DB4 as deposited.

the finishing of the final product if no post fabrication machining is considered.

The deposition dimensions were larger than the CAD model with the tip diameter showing a 27-48 % increase in

dimensions than the CAD model while the shank was 11-22 % larger. The tip length was 2-30 % greater, the flute length 22-27 % less and the total drill bit length 7-8 % longer than the CAD model. The relatively large beam spot size of 1.35 mm meant that any features that were smaller or within 1.35 mm would have poor resolution and the high surface roughness had a more profound effect on the smaller geometry. By reducing the beam spot size, a better resolution will be obtained, but at the cost of longer printing times, hence more powder usage and more laser time. The LENS<sup>TM</sup> machine employed did not allow for simple alteration of the beam size, as it can only be done by manually adjusting the internal lens in the deposition head and testing the new beam spot size. Thus, a large beam size for the shank and a small spot size for the tip is not a viable solution. This indicates that a post processing procedure will be required in majority of cases to comply with strict quality standards.

The best performing drill bit, DB3 as in Table 2, was found to have a circularity and diameter which was within 5% of the commercial drill bit although the hole depth was only 38% of the commercial one. This large variance was due to tip fracture caused by lack of post processing surface smoothing. The von Mises simulations showed that in the designed CAD, Fig. 4(a), and the corrected CAD, Fig. 4(b)-(d), which models the shape of the deposited drill bit, that the highest stress is observed at the base of the tip region. The as-deposited drill bit has a less defined flute and tip which resulted in less of a boring action. A secondary high-stress point is at the top of the shank, due to stress concentrations caused by sharp angles in geometry.

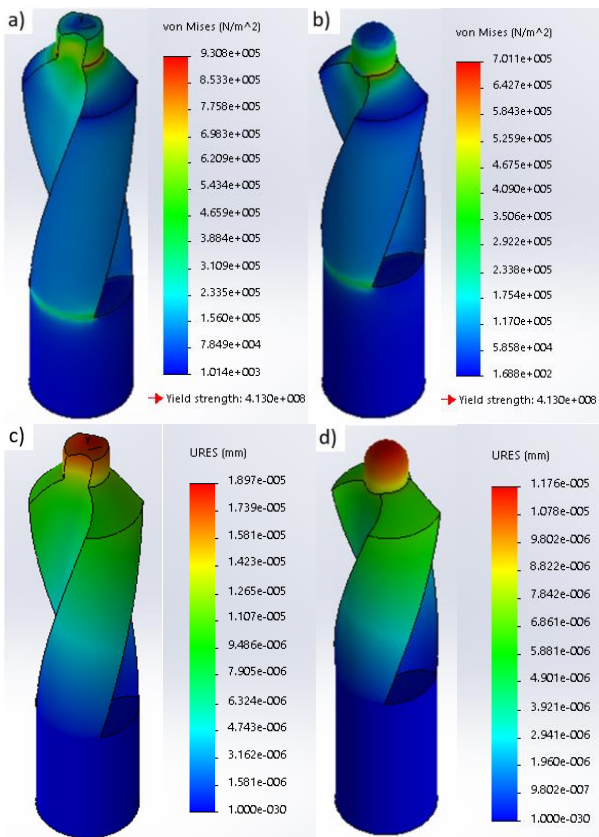


Fig. 4: von Mises stress simulations for a) original cad model, b) as-deposited drill bit and the respective displacement simulations in c) and d).

The highest strain was observed in the tip region, due to the high loading stress, although the displacement is the top region of the tip while the stress is in the base of the tip. The twisted nature of the flute allows for the displacement to be distributed throughout the mass due to its torsional rigidity. The von Mises stress and strain simulations allow for the drill bits to be refined and modified to improve their design properties within the validation phase of the framework.

The manufacturing times were calculated for the experimental phase as well as the optimization phase. The thin walls took a total of 101 minutes of active printing time to complete. Aspects which added to this included the initiation of each new print, refilling the powder hoppers and selecting the next set of process parameters. Since the model for the thin walls remained the same there was no need to change the CAD model, only the process parameters. The three iterations of cubic samples used a total printing time of 22 hours, again without the additional setup and preparation stages. Thus it took approximately 23.5 hours of active printing time to obtain a parameter set which yielded a cube with a density of 97 % without any post printing processes.

The drill bit deposition times varied between 27 minutes and 100 minutes depending on the process parameters which shows that the refinement of parameters can produce time savings of up to 4 times. The cheapest fabricated drill bit was still 3.5 times more expensive than the purchased drill bit. This is due to the entire drill bit comprising of WC-9.2wt% Monel 400 whereas the shank of the purchased drill bit is fabricated from steel and only the tip region from WC based materials. To make the fabricated drill bit competitive the shank should comprise of Monel 400 or steel which is then tipped with a WC-based material, possibly even a functional grading from the steel shank into the tip to remove any adhesion problems between the two dissimilar materials.

#### IV. CONCLUSION

An iterative, multi-phase parameter manufacturing framework was successfully developed and applied to a tungsten carbide alloy having a Monel 400 binder yielding reproducible functional drill bit prototypes after 23.5 hours of active laser time, using the laser engineered net shaping process. The framework provided a systematic process to follow and reduced the need for excessive parameter refinement in attempting to achieve the highest density and production of a component. The framework can be utilised in any experimental setup where a novel material combination is required to be optimised.

The geometries of the fabricated drill bits were larger in every dimension due to the high surface roughness and large spot size used for deposition. The best deposited drill bit produced hole circularity and diameters which were within 5% of the commercial drill bit but was unable to achieve the desired depth due to tip fracture from high stresses and microstructural properties. With suitable post processing machining, the dimensions can be customized and the drill bit performance improved by refining the surface properties by for example heat treatment. The cost of the AM drill bit still greatly exceeds the current conventionally produced commercial product but has its strength in being highly customizable and having short lead times if there is a local additive manufacturing distributor. Although the

commercial drill bit outperformed the prototype bits, the deposition of a competitive drill bit may be possible with a second iteration of parameter refinement, and/or by employing a different geometry.

#### ACKNOWLEDGEMENT

The authors wish to acknowledge the financial support received from the Department of Science and Innovation and the National Research Foundation in South Africa (Grant Nos: 41292 and 129313). The National Laser Centre (NLC) at the Council for Scientific and Industrial Research (CSIR) is acknowledged for use of the LENS® machine as well as technical support (Grant No: LREPA25). Mr. Rodney Gurney is acknowledged for assistance with CNC operation during drill bit testing. Opinions expressed and conclusions arrived at are those of the authors and are not necessarily to be attributed to the funders.

#### REFERENCES

- [1] Y. Xiong, J. E. Smugeresky, and J. M. Schoenung, "The influence of working distance on laser deposited WC-Co," *J. Mater. Process. Technol.*, vol. 209, no. 10, pp. 4935–4941, Jun. 2009, doi: 10.1016/j.jmatprotec.2009.01.016.
- [2] A. Bandyopadhyay, B. V. Krishna, W. Xue, and S. Bose, "Application of Laser Engineered Net Shaping (LENS) to manufacture porous and functionally graded structures for load bearing implants," *J. Mater. Sci. Mater. Med.*, vol. 20, no. S1, pp. 29–34, Dec. 2009, doi: 10.1007/s10856-008-3478-2.
- [3] C. Atwood *et al.*, "Laser Engineered Net Shaping (lens(tm)): A Tool for Direct Fabrication of Metal Parts," Sandia National Laboratories, Albuquerque, NM, and, Livermore, CA, SAND98-2473C, Nov. 1998. Accessed: Apr. 19, 2017. [Online]. Available: <https://www.osti.gov/scitech/biblio/1549>
- [4] M. L. Griffith, L. D. Harwell, J. T. Romero, E. Schlienger, C. L. Atwood, and J. E. Smugeresky, "Multi-material processing by LENS," in *Proceedings of the Solid Freeform Fabrication Symposium*, 1997, pp. 387–393. Accessed: Apr. 06, 2017. [Online]. Available: <http://sffsymposium.engr.utexas.edu/Manuscripts/1997/1997-45-Griffith.pdf>
- [5] T. Gualtieri and A. Bandyopadhyay, "Laser Engineering Net Shaping of Microporous Ti6Al4V Filters," *Front. Mech. Eng.*, vol. 2, 2016, doi: 10.3389/fmech.2016.00009.
- [6] Y. Li, Y. Hu, W. Cong, L. Zhi, and Z. Guo, "Additive manufacturing of alumina using laser engineered net shaping: Effects of deposition variables," *Ceram. Int.*, vol. 43, no. 10, pp. 7768–7775, Jul. 2017, doi: 10.1016/j.ceramint.2017.03.085.
- [7] I. Baturynska, O. Semeniuta, and K. Martinsen, "Optimization of Process Parameters for Powder Bed Fusion Additive Manufacturing by Combination of Machine Learning and Finite Element Method: A Conceptual Framework," *Procedia CIRP*, vol. 67, pp. 227–232, Jan. 2018, doi: 10.1016/j.procir.2017.12.204.
- [8] A. K. Sood, R. K. Ohdar, and S. S. Mahapatra, "Parametric appraisal of fused deposition modelling process using the grey Taguchi method," *Proc. Inst. Mech. Eng. Part B J. Eng. Manuf.*, vol. 224, no. 1, pp. 135–145, Jan. 2010, doi: 10.1243/09544054JEM1565.
- [9] P. K. Jain, P. M. Pandey, and P. V. M. Rao, "Experimental investigations for improving part strength in selective laser sintering," *Virtual Phys. Prototyp.*, vol. 3, no. 3, pp. 177–188, Sep. 2008, doi: 10.1080/17452750802065893.
- [10] H. Bikas, A. K. Lianos, and P. Stavropoulos, "A design framework for additive manufacturing," *Int. J. Adv. Manuf. Technol.*, vol. 103, no. 9–12, pp. 3769–3783, Aug. 2019, doi: 10.1007/s00170-019-03627-z.
- [11] M. Kumke, H. Watschke, and T. Vietor, "A new methodological framework for design for additive manufacturing," *Virtual Phys. Prototyp.*, vol. 11, no. 1, pp. 3–19, Jan. 2016, doi: 10.1080/17452759.2016.1139377.
- [12] K. Salonitis and S. A. Zarban, "Redesign Optimization for Manufacturing Using Additive Layer Techniques," *Procedia CIRP*, vol. 36, pp. 193–198, Jan. 2015, doi: 10.1016/j.procir.2015.01.058.
- [13] Z. Liu, H. Kim, W. Liu, W. Cong, Q. Jiang, and H. Zhang, "Influence of energy density on macro/micro structures and mechanical properties of as-deposited Inconel 718 parts fabricated by laser engineered net shaping," *J. Manuf. Process.*, vol. 42, pp. 96–105, Jun. 2019, doi: 10.1016/j.jmapro.2019.04.020.
- [14] Y. Xiong, J. E. Smugeresky, and J. M. Schoenung, "The influence of working distance on laser deposited WC-Co," *J. Mater. Process. Technol.*, vol. 209, no. 10, pp. 4935–4941, Jun. 2009, doi: 10.1016/j.jmatprotec.2009.01.016.
- [15] Y. Zhai, D. A. Lados, E. J. Brown, and G. N. Vigilante, "Understanding the microstructure and mechanical properties of Ti-6Al-4V and Inconel 718 alloys manufactured by Laser Engineered Net Shaping," *Addit. Manuf.*, vol. 27, pp. 334–344, May 2019, doi: 10.1016/j.addma.2019.02.017.
- [16] D.-S. Shim, G.-Y. Baek, J.-S. Seo, G.-Y. Shin, K.-P. Kim, and K.-Y. Lee, "Effect of layer thickness setting on deposition characteristics in direct energy deposition (DED) process," *Opt. Laser Technol.*, vol. 86, pp. 69–78, Dec. 2016, doi: 10.1016/j.optlastec.2016.07.001.
- [17] D. Liu, S. Q. Zhang, A. Li, and H. M. Wang, "Microstructure and tensile properties of laser melting deposited TiC/TA15 titanium matrix composites," *J. Alloys Compd.*, vol. 485, no. 1, pp. 156–162, Oct. 2009, doi: 10.1016/j.jallcom.2009.05.112.
- [18] J. I. Arrizubieta, A. Lamikiz, M. Cortina, E. Ukar, and A. Alberdi, "Hardness, grain size and porosity formation prediction on the Laser Metal Deposition of AISI 304 stainless steel," *Int. J. Mach. Tools Manuf.*, vol. 135, pp. 53–64, Dec. 2018, doi: 10.1016/j.ijmactools.2018.08.004.
- [19] B. Davoren, N. Sacks, and M. Theron, "Laser engineered net shaping of WC-9.2wt%Ni alloys: A feasibility study," *Int. J. Refract. Met. Hard Mater.*, vol. 86, p. 105136, Jan. 2020, doi: 10.1016/j.jrmhm.2019.105136.
- [20] Y. Huang *et al.*, "Rapid prediction of real-time thermal characteristics, solidification parameters and microstructure in laser directed energy deposition (powder-fed additive manufacturing)," *J. Mater. Process. Technol.*, vol. 274, p. 116286, Dec. 2019, doi: 10.1016/j.jmatprotec.2019.116286.
- [21] T. Amine, J. W. Newkirk, and F. Liou, "Investigation of effect of process parameters on multilayer builds by direct metal deposition," *Appl. Therm. Eng.*, vol. 73, no. 1, pp. 500–511, Dec. 2014, doi: 10.1016/j.applthermaleng.2014.08.005.
- [22] Z. Liu *et al.*, "Feasibility Exploration of Superalloys for AISI 4140 Steel Repairing using Laser Engineered Net Shaping," *Procedia Manuf.*, vol. 10, pp. 912–922, Jan. 2017, doi: 10.1016/j.promfg.2017.07.080.